

## **Applications of Differential Scanning Calorimetry on Materials Subjected by Severe Plastic deformation**

Nong Gao<sup>a</sup>

Materials Research Group, School of Engineering Sciences

University of Southampton, Southampton SO17 1BJ, U.K

[N.Gao@soton.ac.uk](mailto:N.Gao@soton.ac.uk),

**Keywords:** differential scanning calorimetry, DSC, severe plastic deformation, SPD, ECAP, HPT

**Abstract.** Differential Scanning Calorimetry (DSC) is a thermal analysis technique that measures the energy absorbed or released by a sample as a function of temperature or time. DSC has wide application for analysis of solid state reactions and solid-liquid reactions in many different materials. In recent years, DSC has been applied to analyze materials and alloys processed through Severe Plastic Deformation (SPD). The basic principle of SPD processing is that a very high strain is introduced into materials which achieve significant grain refinement and improve properties of materials. This review paper presents some recent examples of the applications of DSC for materials subjected to SPD, especially by Equal-Channel Angular Pressing and High-Pressure Torsion.

### **Introduction**

Differential Scanning Calorimetry (DSC) is a thermo analytical technique in which the difference in the amount of heat required to increase the temperature of a sample and reference are measured as a function of temperature [1]. When reactions occur in the sample, DSC provides a direct calorimetric measurement of the energy released or absorbed at the temperature range of the transition. DSC has been applied extensively to the analysis of various materials, including analysis of solid state reactions, such as precipitation, homogenizing, devitrification and recrystallization; and analysis of solid-liquid reactions such as incipient melting and solidification [1]. There are several particular advantages by using DSC analysis, which include: rapid analysis time; very small sample size, typically 1-20 mg; characterization of thermal transitions that could impact product performance, tracking of material changes, i.e. during manufacturing processes or because of environmental exposure.

Many different severe plastic deformation (SPD) processes have been developed during the last two decades [2]. The major methods for the fabrication of ultrafine-grained (UFG) materials include equal-channel angular pressing (ECAP), high-pressure torsion (HPT), accumulative roll-bonding (ARB). All of these procedures are capable of introducing large plastic straining and significant microstructural refinement in bulk crystalline solids. A unique feature of SPD processing is that the high strain is imposed without any significant change in the overall dimensions of the workpiece [3]. Depending upon the crystal structure, the processed microstructures have grain sizes lying typically within the range of 70–500 nm. UFG metals and alloys processed by SPD techniques have superior mechanical properties, such as high strength with good ductility and excellent superplasticity at lower temperature and higher strain rates [4]. In addition to small grain size, SPD materials also have a high dislocation density and high internal stress and these characteristics tend to make their microstructures thermally unstable. There are many different analytical techniques in analyzing SPD processed materials, including scanning electron microscopy (SEM), electron backscatter diffraction (EBSD) and transmission electron microscopy (TEM). However, as the study of the thermal stability of UFG materials is becoming increasingly important for SPD-processed materials, DSC becomes a more attractive technique.

DSC is a powerful tool for studying the thermal stability of UFG materials which directly relates the energy release to microstructural changes such as dislocation density change and grain growth. In this paper a range of published DSC work on SPD materials are presented.

### DSC application for ECAP processed materials

The thermal stability of the microstructure of pure copper specimens deformed by ECAP up to eight passes was examined by DSC [5]. A broad exothermic peak was observed on the DSC curve for each sample (Fig.1). It was found that the maximum of the exothermic peak in the DSC trace shifted to lower temperature values and the heat released during the annealing increased with the increase of strain up to  $\epsilon = 4$ . These changes were explained by an increase of the stored energy introduced by severe plastic deformation which raises the driving force for nucleation of new strain-free grains, so that nucleation is achieved at lower temperatures [6]. DSC measurements were performed for Cu rods deformed by ECAP up to shear strains  $\gamma \approx 5$  while applying various deformation paths A, B<sub>C</sub> and C [7]. The stored energy was measured as a function of the total number of passes using DSC. This work showed that the total stored energy increases with accumulated strain, only the values for route C exhibit some discontinuities.

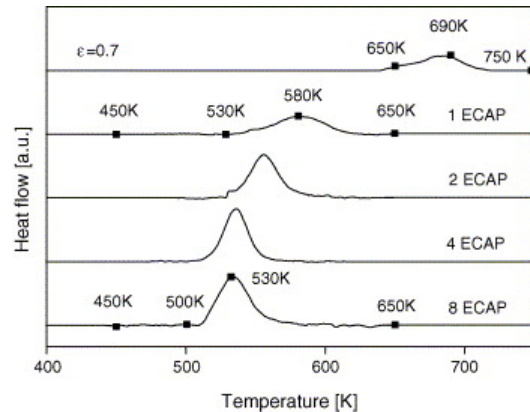


Fig. 1 DSC scans for ECAP deformed Cu specimens [5].

The precipitation and evolution of microstructure in a spray-cast Al-7034 (Al-11.5%Zn-2.5%Mg-0.9%Cu-0.2%Zr) alloy were studied after ECAP using DSC [8]. The major effects in these various regions of Al-7034 alloy were interpreted as GP zone dissolution (I), formation of the  $\eta$ -phase (II), coarsening of the  $\eta$  precipitates (III), dissolution of the  $\eta$ -phase (IV), incipient melting of the T-phase (V) and the onset of full melting of the alloy (VI) (Fig. 2). The similarities in the shapes of the DSC curves after 1, 4 and 8 passes demonstrated that the precipitation processes in the Al-7034 alloy are significantly influenced by the precipitate morphology and specifically by the breaking of the rod-like  $MgZn_2$  precipitates which has been confirmed by TEM to occur mostly in the first pass of ECAP.

Microstructural evolution of ECAP processed and naturally aged ultrafine grained (UFG) and coarse grained (CG) Al-7075 alloys (Al-5.60%Zn-2.50% Mg-1.60%Cu-0.50%Fe-0.40%Si-0.30%Mn-0.23%Cr-0.20%Ti) were investigated by DSC [9]. The sample was processed for two passes by route Bc and DSC analysis in Fig. 3 was at a constant heating rate of 5 or 10 °C/min. The low and high temperature endotherms are due to the GP zone dissolution (I) and the dissolution of the equilibrium  $\eta$  phase (III), and the two exotherms in the intermediate temperature region includes the intermediate metastable phase  $\eta'$  (IIA) and equilibrium phase  $\eta$  formations (IIB). The first endotherm of the CG sample is broader and the peak temperature is about 25 °C lower than that of the UFG sample. The two exothermic peaks of the CG sample overlapped much more than those of the UFG sample. In addition, the first exothermic peak

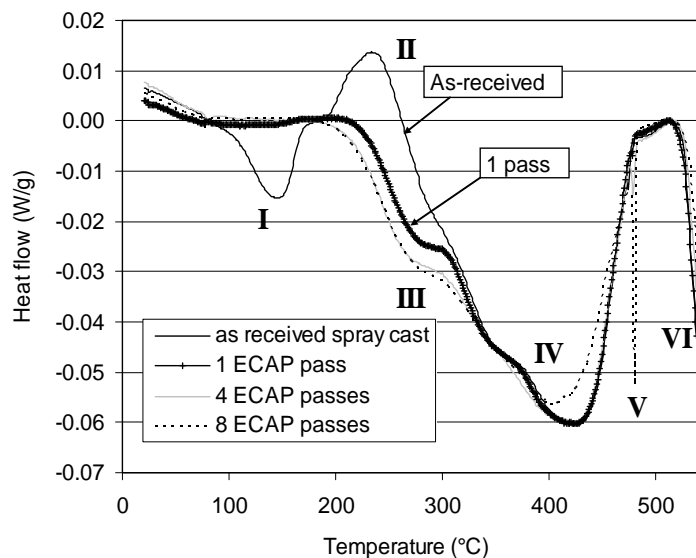


Fig. 2 DSC curves of Al-7034 alloy [8]

temperature of the UFG sample is about 20°C lower than that of the CG sample. The second endotherm of the UFG sample is much broader than that of the CG sample. For the first endotherm,  $\Delta H$  of the UFG sample is equivalent to that of the CG sample. For the exotherms and the second endotherm,  $\Delta H$  of the UFG sample is evidently larger than those of the CG sample. Therefore, DSC analysis indicates that the ECAP process only accelerated the phase precipitations, but did not change the sequence of phase precipitation.

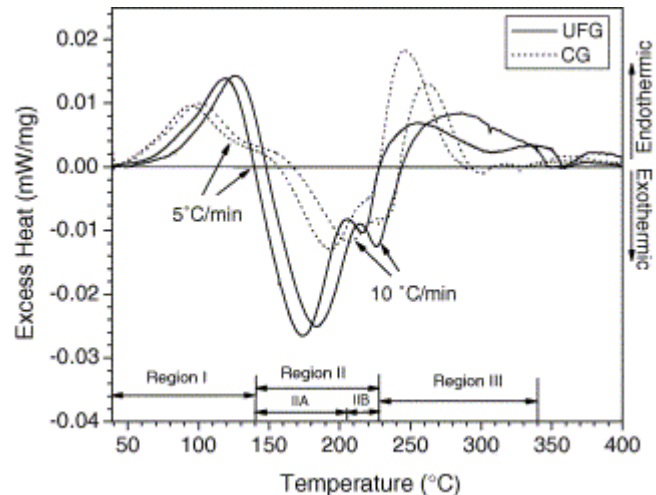


Fig. 3 DSC scans of ultrafine grained (UFG) and coarse grained (CG) samples of Al-7075 alloys [9].

Comparative analyses by DSC were carried out on the ECAP severely deformed Al-Mg-Si (Al-0.34%Mg-0.51%Si-0.16%Fe-0.014%Mn-0.10%Zr) and Al-Mg-Si-Sc (Al-0.36%Mg-0.50%Si-0.14%Fe-0.013%Mn-0.10%Zr-0.12%Sc) alloys to evaluate their ageing behaviour and to exam thermal stability of the grain structure [10]. It was found that the precipitation sequence and kinetics remain substantially the same for the two alloys. The only exception is that the ECAP processed Sc-free samples showed a clear recrystallization peak at temperature in the range 315-360°C whereas the Sc containing alloy retained its ultrafine structure to temperature well exceeding 450°C. It also was demonstrated that severe plastic deformation induces changes of the precipitation kinetics by increasing the diffusivity in the lattice and the density of nucleation sits for precipitates. This effect is confirmed by the shift of the recrystallization peaks toward lower temperatures by increasing the number of ECAP passes of the samples.

DSC has been used to study the effect of the ECAP temperature on the microstructure of the magnesium alloy AM60 (Mg-6%Al-0.13%Mn), with three samples pressed 10 passes at 150, 210 and 350°C (Fig. 4) [11]. In all curves of the ECAPed samples four peaks can be identified. The first peak is located at a temperature of about 150°C. The second peak at about 300°C is absent in the initial as-cast alloy, but present in all the ECAPed samples. Peak 3 occurs at 390°C in the case of the initial alloy and is shifted to lower temperatures (from 385 to 360°C) with decreasing ECAP temperature. Peak 4 appears at the same temperature (about 430°C) in case of all samples. TEM analysis revealed that the third peak is associated with the dissolution of the  $Al_{12}Mg_{17}$  precipitates, and the annealing of ECAP induced dislocations.

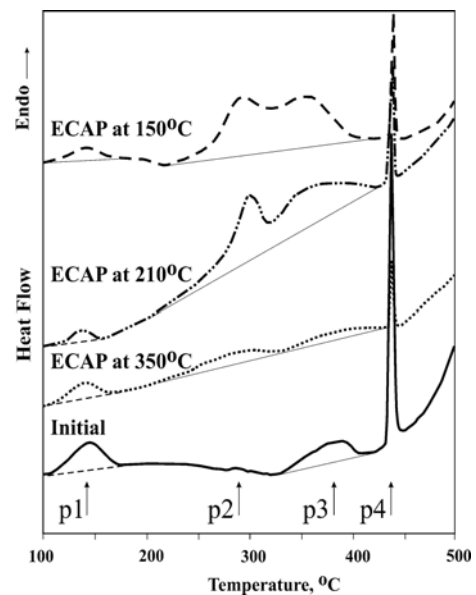


Fig. 4 DSC curves of AM 60 alloys

Effect of high-temperature ECAP on transformation behaviors of Ti-50.3at.%Ni shape memory alloy (SMA) was investigated by DSC measurements [12]. Figure 5(a) showed that two exothermic peaks were observed for the as-received alloy, which were corresponding to the B2 parent phase to the R-phase and then to the martensite phase transformations. During the heating process of the specimen, only one endothermic peak was observed, which revealed that reverse R-phase transformation and reverse martensitic transformation were overlapped together. On the other hand, it was found that there was only one broadened exothermic peak on the cooling curve and the B2 to R-phase transformation peak was unclear after two high-temperature ECAE

processes (Fig. 5(b)). Meanwhile, the transformation temperatures decreased sharply. It is obvious that the severe shear deformation of TiNi matrix during the ECAE process affected the microstructural revolution.

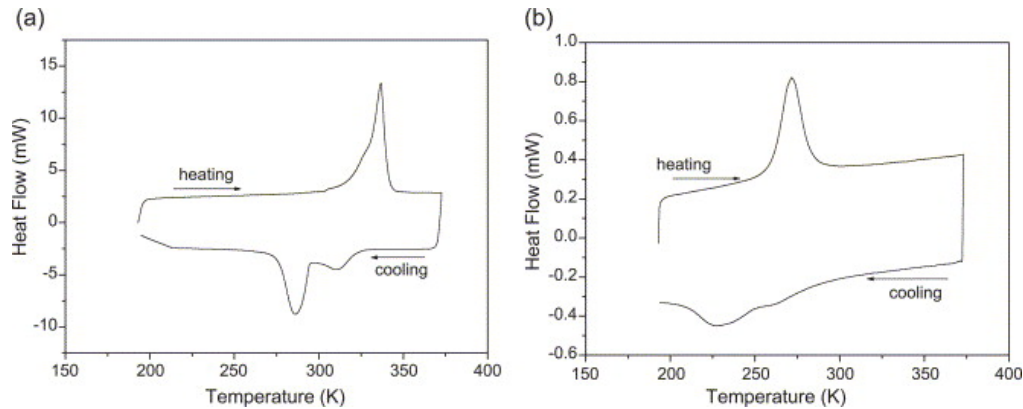


Fig. 5 DSC curves of TiNi alloy before (a) and after (b) two ECAE processes [12].

The morphological changes of isotactic polypropylene (iPP) subjected to varying shear strains by ECAP have been investigated by X-ray scattering and DSC [13]. Enthalpy of fusion,  $\Delta H$ , was determined by integrating the area under the baseline corrected thermogram between 130 and 175°C. Percentage crystallinity was calculated. The DSC experimental results confirm that the crystallinity as measured by DSC ( $\chi_{DSC}$ ) decreased in roughly the same manner to the crystallinity as measured by X-ray (Fig. 6).

### DSC application for HPT and ARB processed materials

Processing UFG by HPT is an especially attractive procedure because, by comparison with ECAP, it leads both to smaller grains and to a higher fraction of high-angle grain boundaries [14]. DSC curves of copper samples (98.51%Cu-1.49%Si) showed that there are two exothermic peaks in each curve for samples processed by HPT with varying turns [15]. The peak at lower temperature range 180–280°C (first peak) is caused by recrystallization. To find out what caused the second peak, DSC runs also were carried out on a coarse-grained sample, which demonstrated that there is an exothermic reaction whose temperature range matches the second exothermic peak. Therefore, it was believed that the second peak was caused by the oxidation of the copper sample. Figure 7 shows energy releases calculated from the first peak from samples processed by HPT for varying turns. It is apparent that the energy release increases and the peak position shifts to lower temperature with increasing HPT turns.

Nickel rods of 99,99% and 99,998% purity have been deformed by HTP at different degrees of pressure (1GPa, 4GPa and 8GPa) and different degrees of shear strain  $\gamma$  from 1 up to 25 [16]. The pure (99.998%) Ni exhibited two exothermic peaks in the heat flow curve (Fig. 8(a)), while the 99.99% Ni reveals only one peak at the higher temperatures (Fig. 8(b)). The two exothermic peaks have been identified to

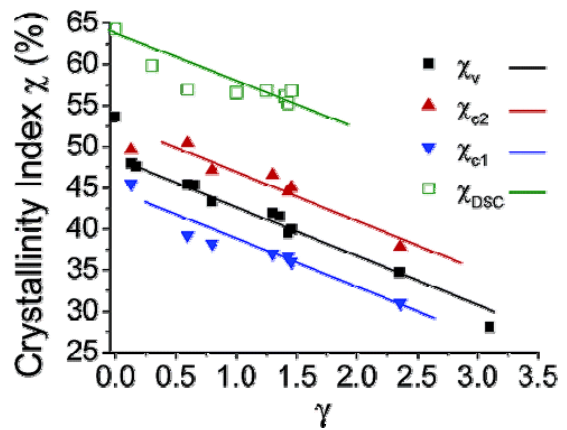


Fig. 6 Plots of crystallinity index as a function of shear strain for isotactic polypropylene [13].

Figure 7 shows energy releases calculated from the first peak from samples processed by HPT for varying turns. It is apparent that the energy release increases and the peak position shifts to lower temperature with increasing HPT turns.

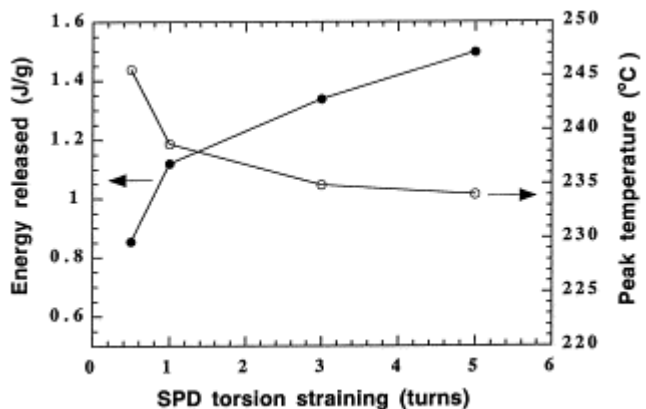


Fig. 7 Energy release and DSC peak shift of HPT processed Cu samples [15].

originate from the annealing of single and/or double vacancies, and dislocations, respectively. It showed that with increasing strain, the dislocation peak shifted to lower temperatures while the temperature of vacancy peak remained more or less constant.

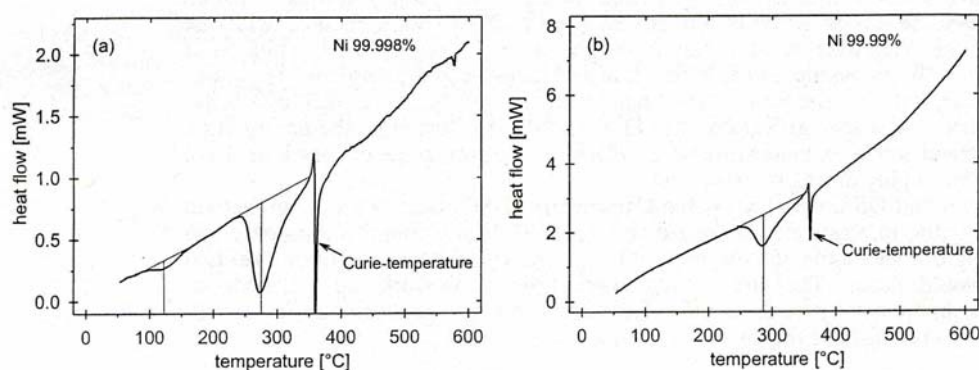


Fig. 8 The DSC curves of the two Ni purities processed by HPT (16).

High pressure torsion straining was applied to  $\text{Al}_{90}\text{Fe}_5\text{Nd}_5$  powders to achieve cold consolidation to full density [17]. Before applying HPT, a broad exotherm was seen between 150 and 270°C (signals precipitation of fcc-Al in the amorphous matrix) followed by a sharp exothermic reaction around 350°C and a weaker one around 570°C. However, DSC thermogram of the  $\text{Al}_{90}\text{Fe}_5\text{Nd}_5$  powder after severe plastic deformation was completely absent the initial exothermic activity (between 150–270°C).

Figure 9 shows DSC curves of 99.99% purity copper ARB processed by various cycles [18]. The exothermic peaks appeared at 210–253°C. The observation of microstructure by EBSD in samples before and after DSC measurements reveals that these peaks were caused by primary recrystallization. The peak positions shifts to lower temperature with increasing strains. This suggested that the evolution of finer microstructure with increase the strain enhanced the occurrence of recrystallization at lower temperature. The stored energy was estimated to range from 43 to 53 J/mol.

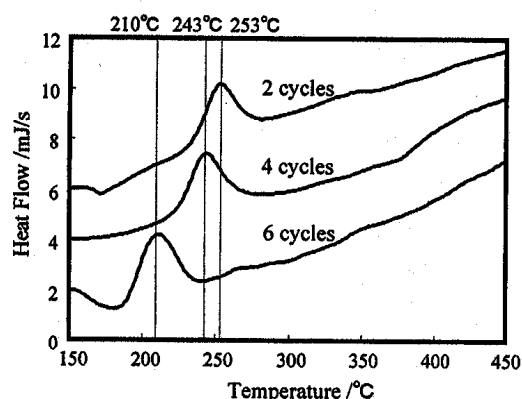


Fig. 9 DSC curves of copper processed by ARB

### Some issues related to DSC analysis

Whilst the advantages of non-isothermal calorimetry experiments of DSC are well known, temperature scanning methods have their own particular drawbacks and difficulties associated with them [1]. Several factors influence the DSC results in accuracy, such as sample preparation, testing condition and baseline correction, which should be carefully handled during DSC analysis. During sample preparation, punching, grinding, machining and cutting all introduce deformation, and this influences precipitation in most heat treatable light alloys by providing sites for heterogeneous nucleation, and by annihilating quenched-in excess vacancies. When using DSC to determine transition temperatures and enthalpy of an alloy, it is necessary to choose what heating and cooling rate to use. The common heating rates used are 10–40°C/min as this gives good resolution without being subject to picking up inordinate amounts of noise. In analyzing linear heating experiments the baseline of the DSC needs to be carefully considered, as baselines will generally be a temperature and time dependent [1,19]. Although DSC is a very valuable and efficient technique to analyze a number of reactions that occur in various materials and light alloys, calorimetry experiment in itself can not identify the phases involved in the reactions. Therefore other techniques, such as high resolution transmission electron microscopy (HREM), transmission electron microscopy (TEM),

electron dispersive X-ray spectroscopy (EDS), scanning electron microscopy (SEM) and X-ray diffraction, should be used to identify these phases. To identify the phase changes unambiguously one would heat a sample to a condition that corresponds to the start of the thermal effect and a second sample would be heat to a condition that corresponds to the end of the thermal effect, and preferably further samples would be heat treated to intermediate stages. These samples would then be analyzed using an analysis technique that provides conclusive information on the phases suspected to be involved in the reaction.

### Summary

DSC, as an effective thermal analysis technique, can be widely used to obtain qualitative information on the state of microstructure and the precipitation sequence. The simplicity and rapid nature of the DSC technique and the general availability of the apparatus make it an economical method of obtaining temperatures of reactions. In recent years, DSC has been increasingly applied to analyze materials and alloys processed through SPD which have provided much useful information. However, the identification of heat effects in the more complex alloys is not straightforward, which will require extensive supporting microstructural investigations.

### Acknowledgement

The author wish to thank Professor M. J. Starink for valuable discussions. The work was funded in part by EPSRC under Grant No. EP/D00313X/1.

### References

- [1] M. J. Starink, *Inter. Mater. Review*. Vol. 49 (2004), p. 191.
- [2] R. Z. Valiev and T. G. Langdon, *Prog. Mater. Sci.* Vol. 51 (2006), p. 881.
- [3] R. Z. Valiev, Y. Estrin, Z. Horita, T. G. Langdon, M. J. Zehetbauer and Y. T. Zhu, *JOM*. Vol. 4 (2006), p. 33.
- [4] K. Matsubara, Y. Miyahara, Z. Horita and T.G. Langdon. *Acta Mater.* Vol. 51 (2003), p. 3073.
- [5] J. Gubicza, L. Balogh, R. J. Hellmig, Y. Estrin and T. Ungar, *Mater. Sci. Eng.* Vol. A400-401 (2005), p. 334.
- [6] Y. M. Wang and E. Ma, *Acta Mater.* Vol. 52 (2004), p. 1699.
- [7] E. Schafler, G. Steiner, E. Korznikova, M. Kerber and M. J. Zehetbauer, *Mater. Sci. Eng.* Vol. A410-411 (2005), p. 169.
- [8] N. Gao, M. J. Starink, M. Furukawa, Z. Horita, C. Xu and T. G. Langdon, *Mater. Sci. Forum*. Vol. 503-504 (2006), p. 275.
- [9] Y. H. Zhao, X. Z. Liao, Z. Jin, R. Z. Valiev and T. T. Zhu, *Acta Mater.* Vol. 52 (2004), p. 4589.
- [10] G. Angella, P. Bassani, A. Tuissi, D. Ripamonti and M. Vedani, *Mater. Sci. Forum*. Vol. 503-504 (2006), p. 493.
- [11] B. Mingler, O. B. Kulyasova, R. K. Islamgaliev, G. Korb, H. P. Karnthaler and M. J. Zehetbauer, *J. Mater. Sci.* Vol. 42 (2007), p. 1477.
- [12] Z. Li, X. Cheng and Q. Shangguan, *Mater. Letters*. Vol. 59 (2005), p. 705.
- [13] A. Phillips, P.-W. Zhu and G. Edward, *Macromolecules* Vol. 39 (2006), p. 5796.
- [14] G. Sakai, Z. Horita and T. G. Langdon, *Mater. Sci. Eng.* Vol. A393 (2005), p. 344.
- [15] H. Jiang, Y. T. Zhu, D. P. Butt, I. V. Alexandrov and T. C. Lowe, *Mater. Sci. Eng.* Vol. A290 (2000), p.128.
- [16] E. Korznikova, E. Schafler, G. Steiner and M. J. Zehetbauer, in: *Ultrafine grained Materials IV*, edited by Y.T. Zhu et al. TMS, Warrendale, PA (2006), p. 97.
- [17] A. R. Yavari, W. J. Botta Filho, C. A. D. Rodrigues, C. Cardoso and R. Z. Valiev, *Scripta Mater.* Vol. 46 (2002), p. 711.
- [18] N. Takata, K. Yamada, K. Ikeda, F. Yoshida, H. Nakashima and N. Tsuji, *Mater. Sci. Forum*. Vol.503-504 (2006), p. 919.
- [19] C. Y. Zahra and A. -M. Zahra, *Thermochimica Acta*, Vol. 276 (1996), p. 161.